

Functional Correspondences in the Human and Marmoset Visual Cortex During Movie Watching: Insights from Correlation, Redundancy, and Synergy

Qiang Li¹, Ting Xu², Vince D. Calhoun¹

¹Tri-Institutional Center for Translational Research in Neuroimaging and Data Science (TReNDS)
Georgia State University, Georgia Institute of Technology, Emory University, Atlanta, GA, United States

²Child Mind Institute, Center for the Integrative Developmental Neuroscience, New York, NY, United States

Abstract

The world of beauty is deeply connected to the visual cortex, as perception often begins with vision in both humans and marmosets. Quantifying functional correspondences in the visual cortex across species can help us understand how information is processed in the primate visual cortex, while also providing deeper insights into human visual cortex functions through the study of marmosets. In this study, we measured pairwise and beyond pairwise correlation, redundancy, and synergy in movie-driven fMRI data across species. Our first key finding was that humans and marmosets exhibited significant overlaps in functional synergy. Second, we observed that the strongest functional correspondences between the human peri-entorhinal and entorhinal cortex (PeEc) and the occipitotemporal higher-level visual regions in the marmoset during movie watching reflected a functional synergistic relationship. These regions are known to correspond to face-selective areas in both species. Third, redundancy measures maintained stable high-order hubs, indicating a steady core of shared information processing, while synergy measures revealed a dynamic shift from low- to high-level visual regions as interaction increased, reflecting adaptive integration. This highlights distinct patterns of information processing across the visual hierarchy. Ultimately, our results reveal the marmoset as a compelling model for investigating visual perception, distinguished by its remarkable functional parallels to the human visual cortex.

Keywords: primate visual cortex; functional correspondences; correlation; redundancy; synergy; high-order hubs

1 Introduction

The visual system is one of the most powerful information-communication bridges between the complex redundancy world and the primate brain. Information processing in the primate visual brain is a key neuroscience and development problem [1]–[5]. Given that directly invasive recordings of human visual neural signals are impossible, and marmoset as one of the standard non-human primate models to study human visual functions has already become one of the standard ways to explore the functionalities of the human visual brain [6]–[9]. Therefore, to understand how information processing in the human brain will be proximate to information processing in the marmoset visual brain. Previous research showed that the visual cortex shared the largest similarity across species [6]–[8], [10].

The complex process of naturalistic information processing in the primate visual brain has a long research history, but the underlying neural mechanisms remain unclear. Fortunately, homology between primate brain regions has been identified in recent studies [6], [11], [12]. As mentioned earlier, studying human visual brain function presents several challenges. To gain a deeper understanding, we can use marmosets as a model for both invasive and non-invasive visual experiments. Identifying shared functionalities across species is crucial, as it provides an opportunity to enhance our understanding of human vision through the marmoset model.

Furthermore, to investigate functional correspondences between humans and marmosets under naturalistic movie stimuli, particularly with complex moving stimuli such as faces, bodies, and scene-related elements, we aim to analyze neural responses and identify shared visual processing mechanisms. This will provide valuable insights into how these stimuli are processed in the brain of both species and reveal similarities and differences in their neural representations. Previous studies have mainly focused on pairwise interactions, which has explained some results [6], [11]. However, these methods are limited as they focus solely on pairwise relationships and may overlook higher-order dependencies [3]–[5]. Moreover, understanding the synergy of information in the brain is crucial, as this aspect is often overlooked when examining functional correspondence across species [10].

To address these limitations, we employ both pairwise and beyond pairwise correlation metrics, along with redundancy and synergy measures, to quantify the functional similarities and differences in the functional magnetic resonance imaging (fMRI) activity within the visual areas of humans and marmosets during movie-watching. This comprehensive approach provides new insights into functional correspondences in the visual cortex of both species that may have been overlooked in previous studies. Our goal is to measure the interaction of information through correlation, redundancy, and synergy among visual regions in response to visual stimuli across species. The redundancy and synergy measures of information distribution across the primate visual cortex offer deeper insights into visual processing mechanisms.

2 Materials and Methods

2.1 Data Acquisition and Preprocessing

We made use of existing open-source functional movie-driven task fMRI datasets [6], which includes 13 human healthy volunteers (9 males and 4 females, 22-56 years old), along with 8 common marmosets (6 males and 2 females, 20 and 42 months old). More details on the scanning parameters and data preprocessing for both species can be found in [6]. As illustrated in Fig. 1, 26 visual areas in humans and 25 areas in marmosets were identified during naturalistic movie stimuli. These visual areas exhibited varying degrees of activation in response to movie stimuli, particularly those related to face, body, and scene patches, across both human and marmoset visual cortex. Using the multimodal cortical parcellation atlas [13] for humans and the Paxinos atlas [14] for marmosets, the time courses were extracted from all activated regions of interest (ROIs) in both species.

2.2 Theoretical Analysis

2.2.1 Correlation

Pairwise Relationship Measures with Cross-Correlation

Letting $x_i(t)$ and $y_j(t)$ represent the fMRI signals for two visual regions x_i and y_j at time point $t(t = 1, \dots, T)$, then cross-correlation [15] will be denoted as,

$$\rho_{cc}(x_i(t), y_j(t)) = \rho_{x_i(t)y_j(t)}(m) = \begin{cases} \sum_{i=0}^{t-m-1} x_{i+m}(t) y_j^*(t) & \text{if } m \geq 0 \\ \rho_{y_j(t)x_i(t)}(-m) & \text{if } m < 0 \end{cases} \quad (1)$$

where y_j^* represents the complex conjugate of y_j . Index m represents the displacement between the two signals and is referred to as a lag or lead depending on whether it takes on a positive or negative value. The cross-correlation generates a vector of similarity measures for each value of m , whereas instantaneous correlation generates a single measure. This could be useful in identifying visual brain regions that are not functionally connected at the same time but become functional after a delay.

Multi-way Relationship Measures with Multi-Correlation

To quantify interactions beyond pairwise relationships in the data, we applied multi-correlation, which captures interactions among multiple variables, estimated through linear fitting of the pairwise data [16].

$$1 - \lambda(R') \quad (2)$$

where R' denotes a minor of R and λ represents the smallest eigenvalue of the visual connectivity matrix. The strength of linear relationships between the random variables is determined by this measure. To compute each multi-correlation measure for k -way ($k > 2$) interactions among n variables, we iterate over each set of indices used to extract minors of R . For each minor, the multi-correlation is computed according to Eq. 2. In total, there are $\binom{n}{k}$ possible sets of interactions from the input complex signals.

To represent high-order interactions in a pairwise manner, we first construct a hypergraph where nodes represent visual regions, and hyperedges capture multi-region interactions. Since hypergraphs encode complex

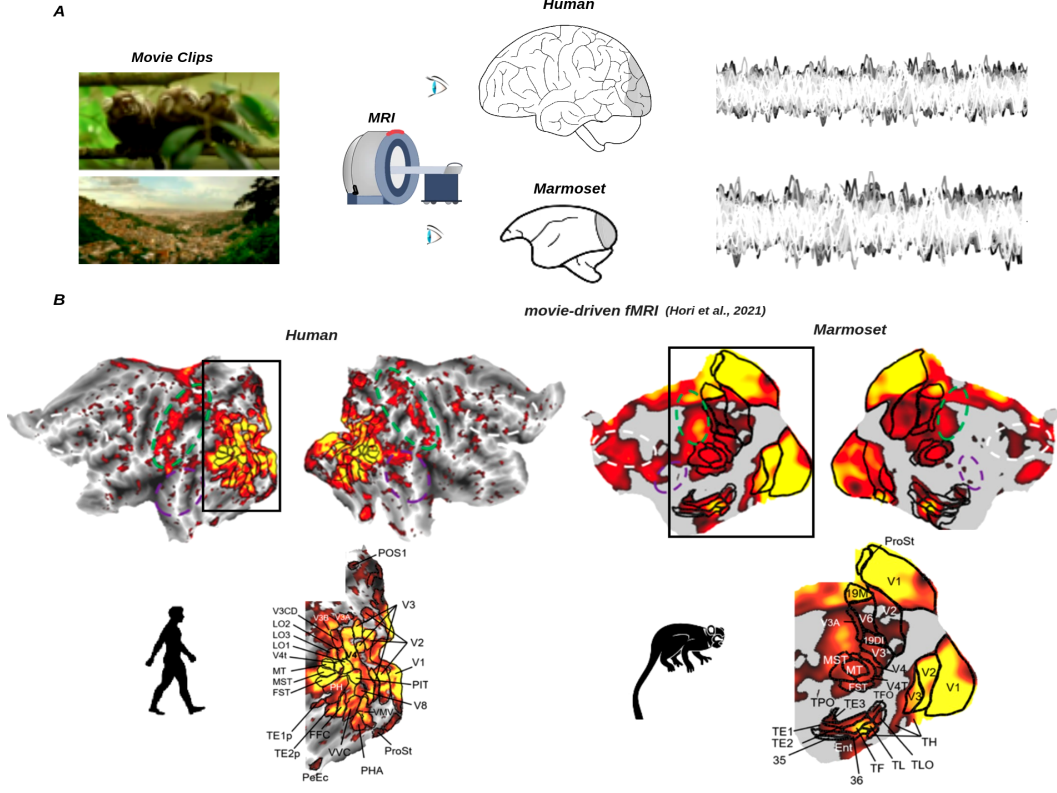


Figure 1: The aligned activated visual cortex between humans and marmosets during naturalistic movie stimuli. **A.** Naturalistic movie stimuli were presented to both humans and marmosets while brain activity was recorded using an magnetic resonance imaging (MRI) machine. After preprocessing, time courses from the activated visual regions were extracted. **B.** The aligned activated visual cortex in humans and marmosets during naturalistic movie stimuli is presented. In the human visual cortex, 26 visual regions are labeled, while 25 visual regions are labeled in the marmoset visual cortex. The flat cortical maps of the human and marmoset brains were adapted from [6].

relationships beyond pairwise connections, we convert the hypergraph into a clique, where each hyperedge is transformed into fully connected subgraphs. This conversion allows high-order interactions to be analyzed using traditional graph-based methods while preserving critical multi-region dependencies [17].

2.2.2 Redundancy and Synergy

Partial Information Decomposition

The partial information decomposition (PID) reveals the mutual information that two source variables X and Y provide about a third target variable Z , $I(X, Y; Z)$, can be decomposed into different types of information: information provided by one source but not the other (unique information), information provided by both sources separately (redundant information), or jointly by their combination (synergistic information) [18]. It can be mathematically expressed as,

$$I(X, Y; Z) = \mathbf{R}(X, Y; Z) + \mathbf{U}(X; Z | Y) + \mathbf{U}(Y; Z | X) + \mathbf{S}(X, Y; Z) \quad (3)$$

Where $\mathbf{R}(X, Y; Z)$ refers to redundancy information, $\mathbf{U}(X; Z | Y)$, $\mathbf{U}(Y; Z | X)$ indicates unique information from Y and X , respectively, and $\mathbf{S}(X, Y; Z)$ refers to synergy information. These different approaches offer a more detailed suite of metrics to quantify the complex system. However, limitations remain in applying this framework to dynamic system with temporal dependencies such as brain activation.

Integrated Information Decomposition

To address this challenge and access the redundancy and synergy for brain data, the Integrated Information Decomposition (Φ ID) was developed to extend PID to measure the time-delayed mutual information taking into account both past and current states of brain signal [10], [19]–[21], i.e., $\mathbf{I}(X_{t-\tau}^i, X_{t-\tau}^j; X_t^i, X_t^j)$, where $X_{t-\tau}^i, X_{t-\tau}^j$ refers to past states of brain signal and X_t^i, X_t^j refers to current states. Redundancy, synergy, and unique information can be calculated under the Φ ID framework. In this study, we utilized the Gaussian solver implemented in the Java information dynamics toolkit to compute all information-theoretic quantities using Φ ID [22].

3 Results

3.1 Functional Synergy Reveals Face-Selective Region Connections in Humans and Marmosets

In Fig. 2, intra-species functional correspondences are presented. Firstly, we notice that the cross-correlation and redundancy measures reveal a high similarity in connection patterns, while the synergy measure provides different connection information in both species. Specifically, we find that in the human visual cortex, the perirhinal-entorhinal cortex (PeEc) and temporal area 1 posterior (TE1p) show stronger functional synergy than other connections, which are missed in the correlation and redundancy measures. Secondly, in the marmoset visual cortex, temporal area TF, the occipital part (TFO), and area 36 (A36) show strong functional synergy connections compared to other regions. Finally, we observe that both species share similar connection patterns in the visual brain during movie-watching. For example, the visual brain shows strong functional synergy connections in both species, and low- and middle-level visual regions exhibit stronger connections than high-level visual regions in redundancy measures.

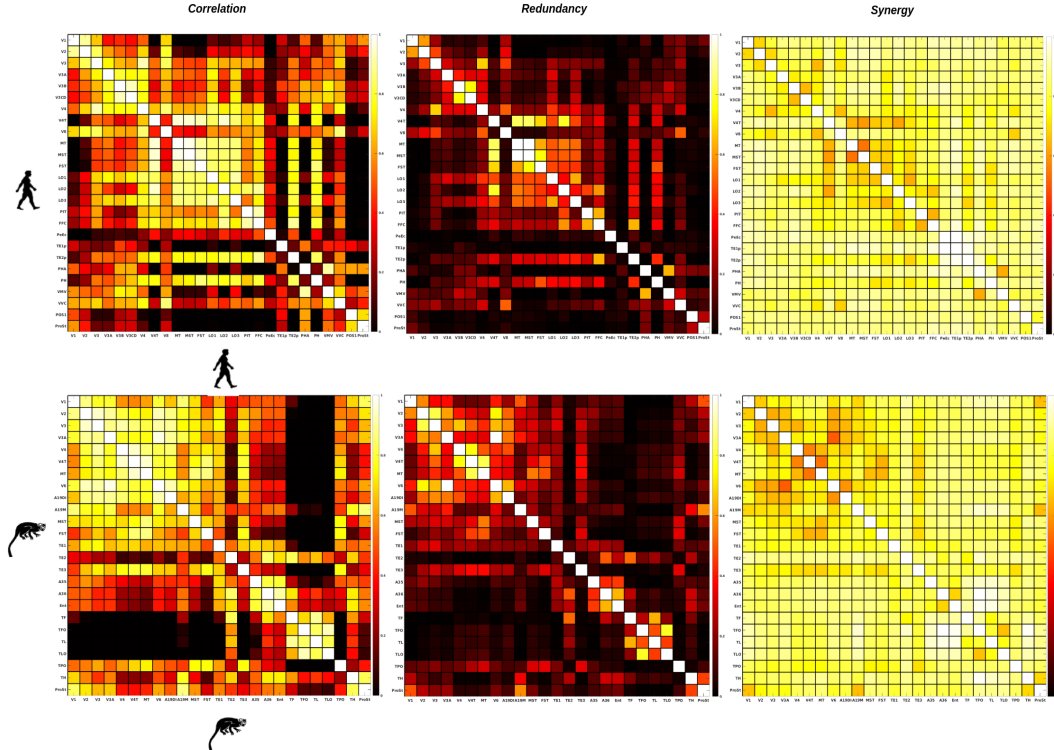


Figure 2: Intra-species functional correspondences were measured using correlation, redundancy, and synergy in both humans and marmosets. The top row presents the human visual cortex correlation matrix based on these measures, while the second row shows the corresponding matrix for the marmoset visual cortex.

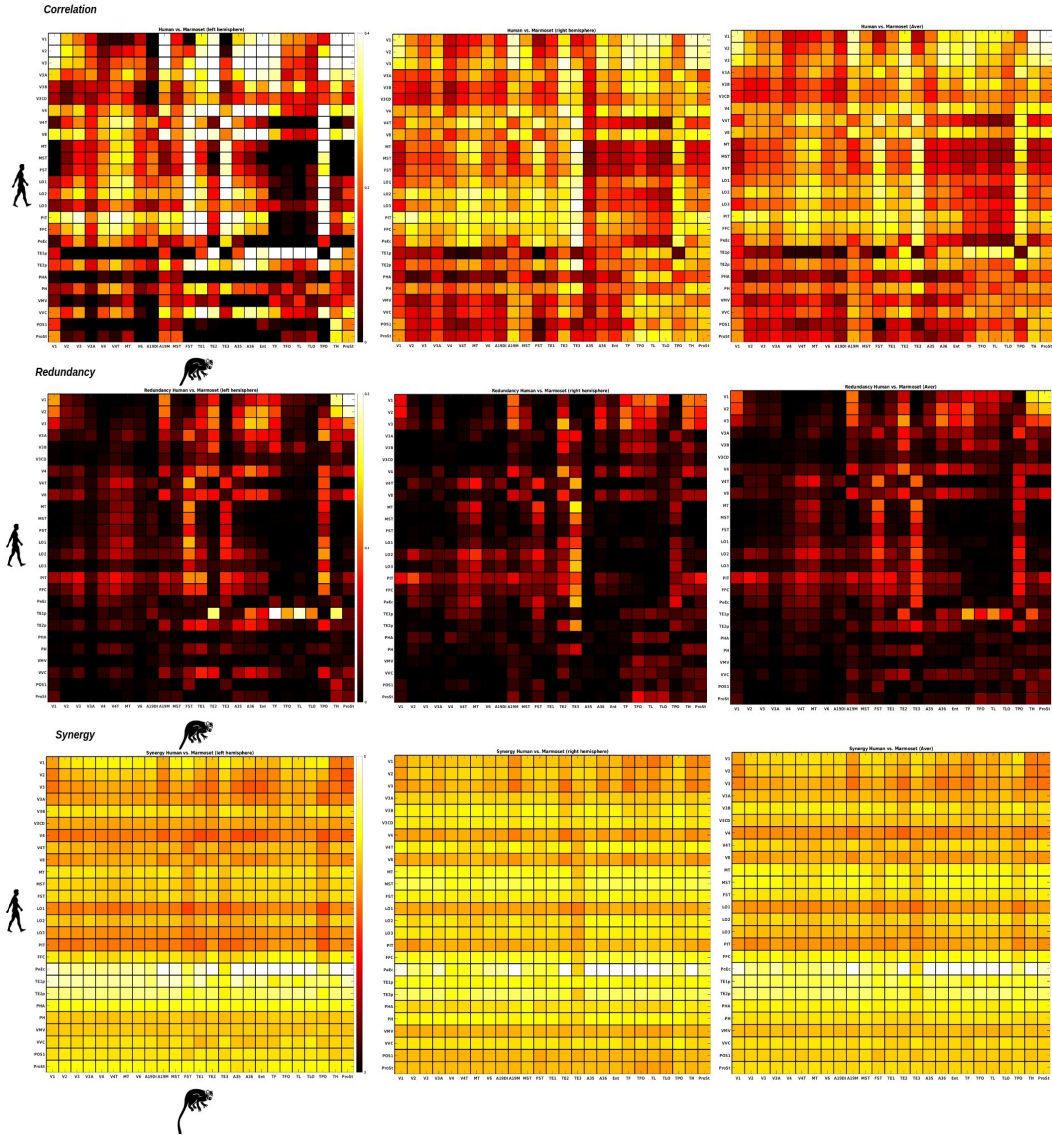


Figure 3: Inter-species functional correspondences were measured using correlation, redundancy, and synergy in the aligned visual cortex of humans and marmosets. The top row presents cross-correlation, displaying results for the left hemisphere, right hemisphere, and their average from left to right. The second row shows redundancy, while the final row illustrates synergy shared between the human and marmoset visual cortex.

3.2 Stronger Functional Synergy in Human PeEc and Marmoset Occipitotemporal Visual Regions

In Fig.3, inter-species functional correspondences are presented. Firstly, the top row shows the cross-correlation similarities between human and marmoset in the left hemisphere, right hemisphere, and average left and right hemisphere, from left to right, and then in the middle row shows the similarities, which were measured using redundancy, and it mostly shows similarity patterns compared to cross-correlation, and they both capture the strongest similarities in brain regions across human and marmoset visual cortex. Furthermore, the synergistic similarities were found between humans and marmosets, and we clearly see that synergy across primate visual cortex has totally different patterns compared to correlation and redundancy. We see that humans and marmoset have large functional overlap in the high-level visual regions, and PeEc regions show the strongest functional similarities with marmoset occipitotemporal high-level visual regions (i.e., A35, A36, Ent, TF, TFO, TL, TLO, and TH). We suggest that these visual regions play a crucial role in comparative primate visual functions under complex naturalistic stimuli, particularly face-related stimuli.

To further assess the relationship between cross correlation, redundancy, and synergy, we examined the relationships between each pair of measurements, as shown in Fig.4. The correlation between cross correlation and redundancy is $r = 0.81$, $p = 1.5904e-155$, while the correlation between redundancy and synergy is $r = -0.36$, $p = 5.0476e-21$, and the correlation between cross correlation and synergy is $r = -0.42$, $p = 1.1161e-29$. These results show that cross correlation and redundancy share the strongest relationship compared to the other pairs.

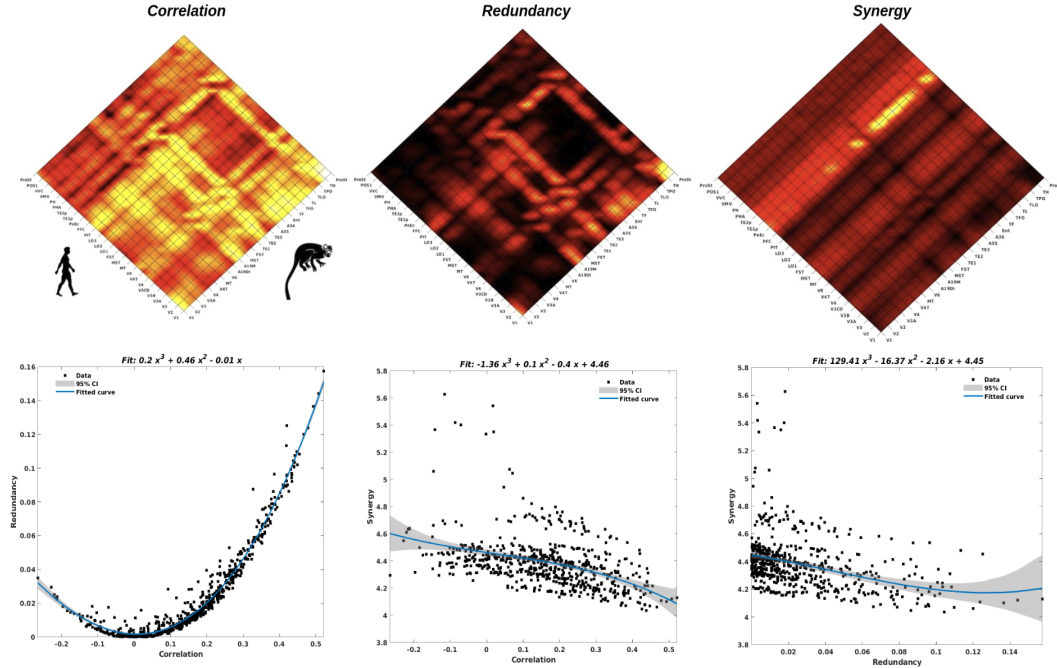


Figure 4: The correlation, redundancy, and synergy statistics were evaluated in the aligned visual cortex of humans and marmosets. The top row shows cross correlation, redundancy, and synergy from left to right. The second row illustrates the relationships between redundancy and cross-correlation, synergy and cross-correlation, and synergy and redundancy.

3.3 High-Order Hubs in the Visual Cortex of Humans and Marmosets

The high-order hubs identified in the visual cortex of humans and marmosets, as illustrated in Fig.5, were estimated using beyond pairwise interactions with interaction orders $k = 3$ and $k = 4$. To better interpret these interactions, we transformed hypergraph-based multi-region connections into pairwise representations. This approach enabled us to systematically identify critical high-order hubs in both species. Notably, redundancy measures preserved stable high-order hubs, while synergy measures revealed a dynamic transition from low- to high-level visual regions as more regions interacted, highlighting differences in information integration across the visual hierarchy.

From redundancy measures, we identified high-order hubs such as MST, MT, and V4T in the human visual cortex, while in marmosets, V6, V3A, and V2 were prominent. In synergy measures, for $k = 3$, high-order hubs in humans included V1, V2, V3, V3A, and V3B, which then shifted to PeEc, TE1p, TE2p, and MT at

$k = 4$. Similarly, in marmosets, high-order hubs initially included V1, V2, V3, V3A, V4, V4T, V6, and MT but transitioned to higher-level visual regions such as TFO, A36, TE2, TH, and Ent. This transition aligns well with interspecies synergy measures, highlighting cross-species functional synergy similarities in visual processing and reflecting the mechanisms of visual information processing.

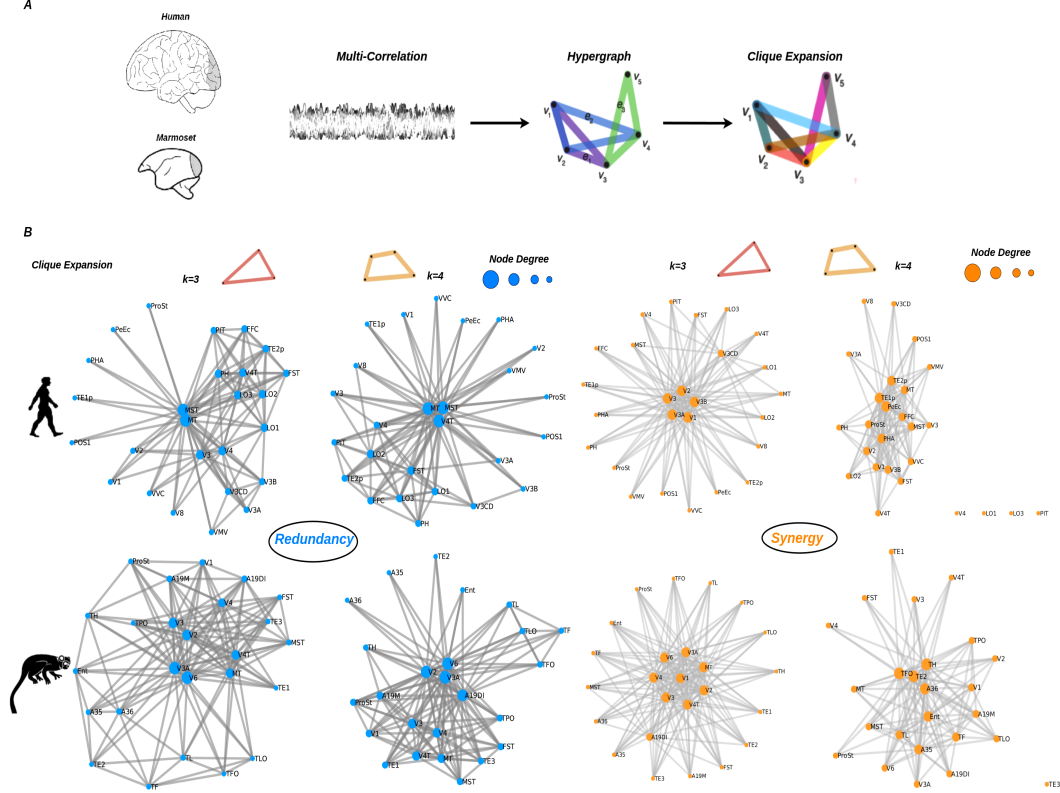


Figure 5: High-Order hubs in human and marmoset brains. **A.** Multi-correlation was estimated from visual neural signals, followed by the construction of a hypergraph that captures beyond pairwise interactions. To facilitate the identification of high-order hubs in both species, the hypergraph was then transformed into a clique representation. **B.** We examined third-order ($k=3$) and fourth-order ($k=4$) interactions in both species and visualized high-order functional connectivity using a force-layout graph. In this representation, redundancy and synergy connections are distinguished, while node size reflects node degree, highlighting key high-order hubs.

4 Discussion

Functional correspondence across species offer valuable insights into the neural mechanisms of visual processing. Comparing how different species handle similar stimuli reveals the evolution of brain function, shared neural representations, and the roles of specific brain regions in visual perception. These insights connect species-specific and universal visual processing pathways, enhancing our understanding of brain functionality across primates [6]. In this study, we assessed functional correspondences in the visual cortex of humans and marmosets by employing pairwise and beyond pairwise correlation, redundancy, and synergy metrics. These measures quantified the information shared across species during exposure to identical movie-based visual stimuli. The findings provided deeper insights into information interactions within the primate visual cortex and further evidence of visual processing mechanisms under these stimuli.

From functional synergy measures, we observed particularly strong connections between regions within intra-species functional correspondences. In the human visual cortex, the PeEc and TE1p demonstrated particularly strong functional synergy. These regions are known for their involvement in visual working memory and higher-level visual processing. Interestingly, both PeEc and TE1p are specifically activated during facial recognition tasks, highlighting their role in processing face-related stimuli [6], [23], [24]. This suggests that these regions not only play a crucial part in general visual perception but may also be specialized for face processing, reinforcing the idea of specialized face-selective networks in the human brain.

In the marmoset, similar functional synergy patterns were observed, particularly between TFO and A36. TFO is known to integrate visual information from various cortical regions, acting as a hub for the coordination of visual processing across different visual domains [25]. This integration suggests that TFO plays a key role in linking low-level visual features with more complex visual representations (such as object and face recognition) [25], [26]. A36, like PeEc in humans, is also a face-selective region in marmosets [11], [27]. Therefore, the strong connection between TFO and A36 may underscore the integration of both low-level and high-level visual information necessary for complex visual tasks, such as object recognition and face perception.

Moreover, TFO’s activation by condition-specific movies, such as the Grasping Hand condition [28], further emphasizes its role in processing dynamic and action-related stimuli. This suggests that TFO is not just involved in static visual processing but also plays a critical role in perceiving and interpreting dynamic visual information, such as movements and actions, which are essential for understanding social and environmental interactions.

By comparing the functional correspondences between these regions in humans and marmosets, we gain insight into the evolutionary conservation of visual processing mechanisms. The shared involvement of regions like PeEc, TE1p, TFO, and A36 in both species highlights the fundamental neural networks that support complex visual functions, particularly related to face and action recognition. Understanding these functional similarities across species helps us appreciate how visual information is processed in the brain, revealing both shared and species-specific mechanisms that are crucial for perception, cognition, and behavior.

From the interspecies functional correspondences analysis, we observed stronger functional synergy in the human PeEc and marmoset occipitotemporal visual regions. The PeEc in humans and the occipitotemporal regions in marmosets are both critical for visual perception, specifically in recognizing and processing faces [6], [11], [23], [24], [26], [27]. This alignment across species suggests that these brain areas play a conserved role in face perception, highlighting the evolutionary stability of face-selective processing mechanisms. Furthermore, the functional synergy between these regions emphasizes their collective involvement in the integration of visual information from multiple sources, which is essential for complex visual tasks like face recognition.

To further examine the functional correspondence in human and marmoset visual cortex, we found that redundancy measures preserved stable high-order hubs, suggesting a robust backbone of overlapping information processing that supports the visual system’s hierarchical structure across species. In contrast, synergy measures revealed a dynamic transition from low- to high-level visual regions as more regions interacted, underscoring an adaptive integration of specialized inputs that evolves with network complexity. This duality highlights not only differences in how information is integrated across the visual hierarchy but also potential evolutionary divergences in cortical strategies for balancing stability and flexibility in perception.

In summary, our findings highlight the potential of the marmoset as a powerful model for visual perception, as it shares a substantial functional correspondence with the human visual cortex.

5 Data Availability

The open-source fMRI shared in previous research [6]. We thank Hori et al. for providing the open-source data used in this study, which was crucial for our analysis.

6 Author Contributions

Qiang Li: Conceptualization; Formal analysis; Visualization; Writing - Original Draft. Ting Xu: Writing - Review & Editing. Vince D. Calhoun: Writing - Review & Editing.

7 Funding Information

This work received no financial support.

References

- [1] S. Watanabe, “Information theoretical analysis of multivariate correlation,” *IBM Journal of research and development*, vol. 4, no. 1, pp. 66–82, 1960.
- [2] A. Rényi, “On measures of entropy and information,” in *Proceedings of the Fourth Berkeley Symposium on Mathematical Statistics and Probability, Volume 1: Contributions to the Theory of Statistics*, University of California Press, vol. 4, 1961, pp. 547–562.
- [3] Q. Li, “Functional connectivity inference from fmri data using multivariate information measures,” *Neural Networks*, vol. 146, pp. 85–97, 2022.

- [4] T. F. Varley, M. Pope, J. Faskowitz, and O. Sporns, “Multivariate information theory uncovers synergistic subsystems of the human cerebral cortex,” *Communications Biology*, vol. 6, 2022.
- [5] Q. Li, G. Ver Steeg, and J. Malo, “Functional connectivity via total correlation: Analytical results in visual areas,” *Neurocomputing*, vol. 571, p. 127 143, Dec. 2023.
- [6] Y. Hori, J. Cléry, J. Selvanayagam, *et al.*, “Interspecies activation correlations reveal functional correspondences between marmoset and human brain areas,” *Proceedings of the National Academy of Sciences of the United States of America*, vol. 118, Sep. 2021.
- [7] Q. Li, V. Calhoun, and A. Iraj, “Revealing complex functional topology brain network correspondences between humans and marmosets,” *Neuroscience Letters*, vol. 822, p. 137 624, Jan. 2024.
- [8] A. Kell, S. Bokor, Y.-N. Jeon, T. Toosi, and E. Issa, “Marmoset core visual object recognition behavior is comparable to that of macaques and humans,” *iScience*, vol. 26, p. 105 788, Dec. 2022.
- [9] J. Mitchell, J. Reynolds, and C. Miller, “Active vision in marmosets: A model system for visual neuroscience,” *The Journal of neuroscience : the official journal of the Society for Neuroscience*, vol. 34, pp. 1183–94, Jan. 2014.
- [10] A. I. Luppi, P. A. Mediano, F. E. Rosas, *et al.*, “A synergistic core for human brain evolution and cognition,” *Nature Neuroscience*, vol. 25, no. 6, pp. 771–782, 2022.
- [11] D. Schaeffer, J. Selvanayagam, K. Johnston, R. Menon, W. Freiwald, and S. Everling, “Face selective patches in marmoset frontal cortex,” *Nature Communications*, vol. 11, p. 4856, Sep. 2020.
- [12] K. Gilbert, J. Cléry, S. Gati, *et al.*, “Simultaneous functional mri of two awake marmosets,” *Nature Communications*, vol. 12, p. 6608, Nov. 2021.
- [13] M. F. Glasser, T. S. Coalson, E. C. Robinson, *et al.*, “A multi-modal parcellation of human cerebral cortex,” *Nature*, vol. 536, no. 7615, pp. 171–178, 2016.
- [14] G. Paxinos, *The Marmoset Brain in Stereotaxic Coordinates*. Elsevier Academic Press, 2012.
- [15] L. R. Rabiner and R. W. Schafer, *Digital Processing of Speech Signals* (Signal Processing Series). Upper Saddle River, NJ: Prentice Hall, 1978, pp. 147–148, ISBN: 0132136031.
- [16] Z. Drezner, “Multirelation—a correlation among more than two variables,” *Computational Statistics & Data Analysis*, vol. 19, pp. 283–292, 1995.
- [17] J. Pickard, C. Chen, R. Salman, *et al.*, “Hat: Hypergraph analysis toolbox,” *PLOS Computational Biology*, vol. 19, no. 6, pp. 1–7, Jun. 2023.
- [18] P. L. Williams and R. D. Beer, “Nonnegative decomposition of multivariate information,” *ArXiv*, 2010. arXiv: [1004.2515](https://arxiv.org/abs/1004.2515).
- [19] P. A. M. Mediano, F. E. Rosas, A. I. Luppi, *et al.*, *Towards an extended taxonomy of information dynamics via integrated information decomposition*, 2021. arXiv: [2109.13186](https://arxiv.org/abs/2109.13186).
- [20] A. B. Barrett and A. K. Seth, “Practical measures of integrated information for time-series data,” *PLoS Computational Biology*, vol. 7, 2011.
- [21] D. Albers and G. Hripcsak, “Estimation of time-delayed mutual information and bias for irregularly and sparsely sampled time-series,” *Chaos, solitons, and fractals*, vol. 45, pp. 853–860, Jun. 2012.
- [22] J. Lizier, “Jidt: An information-theoretic toolkit for studying the dynamics of complex systems,” *Frontiers in Robotics and AI*, vol. 1, Aug. 2014.
- [23] D. Y. Tsao, S. Moeller, and W. A. Freiwald, “Comparing face patch systems in macaques and humans,” *Proc. Natl. Acad. Sci. U.S.A.*, vol. 105, pp. 19 514–19 519, 2008.
- [24] R. Rajimehr, J. C. Young, and R. B. H. Tootell, “An anterior temporal face patch in human cortex, predicted by macaque maps,” *Proc. Natl. Acad. Sci. U.S.A.*, vol. 106, pp. 1995–2000, 2009.
- [25] J. Cléry, D. Schaeffer, Y. Hori, *et al.*, “Looming and receding visual networks in awake marmosets investigated with fmri,” *NeuroImage*, vol. 215, p. 116 815, Apr. 2020.
- [26] A. Dureux, A. Zanini, and S. Everling, “Mapping of facial and vocal processing in common marmosets with ultra-high field fmri,” *Communications Biology*, vol. 7, Mar. 2024.
- [27] C. C. Hung, C. C. Yen, J. L. Ciuchta, *et al.*, “Functional mapping of face-selective regions in the extrastriate visual cortex of the marmoset,” *Journal of Neuroscience*, vol. 35, no. 3, pp. 1160–1172, 2015.

- [28] A. Zanini, A. Dureux, J. Selvanayagam, *et al.*, “Ultra-high field fmri identifies an action-observation network in the common marmoset,” *Commun Biol*, vol. 6, p. 553, 2023.